



Electrochemical MoO_x/Carbon Nanocomposite-Based Gas Sensor for Formaldehyde Detection at Room Temperature

A nanocomposite comprised of molybdenum oxide and highly conductive carbon (MoO_x/Carbon) was deposited onto a screen-printed gold electrode (SPGE) to be employed as a gas sensor for the detection of formaldehyde gas. First, the carbon surface was modified by acid treatment to introduce oxygen-containing groups and promote the efficient anchorage of the molybdenum precursor by surface organometallic chemistry (SOMC). Then, once the MoO_x/Carbon composite was deposited onto the SPGE, a Nafion layer was added to act as a solid-state ionic electrolyte. Fourier-transform infrared (FTIR) spectroscopy and thermogravimetric analysis (TGA) were used to verify the carboxylated surface of carbon after the acid treatment. Scanning transmission electron microscopy (STEM), energy-dispersive X-ray spectroscopy (EDS), X-ray photoelectron spectrosand inductively coupled plasma optical emission spectrometry (ICP-OES) were also employed to confirm the success of the SOMC synthesis. Cyclic voltammetry (CV) and electrochemical impedance spectroscopy (EIS) were used to investigate the interaction of the nanocomposite with formaldehyde at room temperature. The nanocomposite gas sensor showed an enhanced electrical current response when increasing the concentration of formaldehyde, with a limit of detection as low as 60 ppb and sensitivity of 5.13 µA ppm⁻¹. Additionally, the nanocomposite sensor demonstrated high selectivity to formaldehyde when compared to other volatile organic compounds (VOCs).

© 2021 The Electrochemical Society ("ECS"). Published on behalf of ECS by IOP Publishing Limited. [DOI: 10.1149/1945-7111/ac0d3c]

Manuscript submitted April 17, 2021; revised manuscript received June 16, 2021. Published June 28, 2021.

Supplementary material for this article is available online

Volatile organic compounds (VOCs) are chemicals that have a high vapor pressure at ambient temperature, and they often affect human health negatively in long- and short-term upon prolonged exposure for times longer than those indicated by the World Health Organization (WHO). Agriculture, transportation, and industrial processes are some of the emission sources of VOCs.² VOCs are also found as ingredients in construction materials and household products, such as paints, carpets, and cleaning products.³ Since VOCs are harmful chemicals that can be easily found in different setups, various techniques for the detection of VOCs in the gas phase have been intensively studied and developed, such as those based on gas chromatography, spectrophotometry, sion chromatography, and metal oxide semiconductors (MOSs). Since MOS-based gas sensors are relatively simple, cost effective, and require low maintenance, 9,10 these devices have been globally recognized for the detection and measurement of VOCs in the atmosphere. It is notable that MOS sensors are capable of detecting VOCs under various practical field conditions, such as inside buildings, car interiors, storage warehouses, and laboratories. 11 Furthermore, MOS-based gas sensors are able to detect VOCs at concentrations as low as parts per million (ppm) or even parts per billion (ppb), 12-16 and the sensitivity is closely related to the exposed surface area of the metal oxide semiconductor sensing element. Tin (IV) oxide (SnO_2) , 17,18 indium (III) oxide (In_2O_3) , 19 zinc oxide (ZnO), $^{20-22}$ nickel oxide (NiO), and titanium dioxide (TiO₂)²³ are some of the MOSs that have been reported in the literature for the detection of VOCs using electrochemical methods.

Formaldehyde, CH₂O (FA) is classified as one of the most toxic carcinogens by both the WHO and the United States Environmental Protection Agency (US EPA). ^{1,24} Since formaldehyde gas can damage the nervous and immune systems, the WHO has set a maximum of 30 min of exposure to 0.08 ppm of formaldehyde gas to minimize the risk of health issues. ¹ One of the most interesting approaches for the development of gas sensors is the integration of metal oxides and polymers, ^{25,26} and molybdenum oxide (MoO₃) has proven to be a promising sensing element for the detection of

formaldehyde gas. ²⁷ For example, Itoh et al. reported an organic/MoO₃ hybrid gas sensor with high selectivity towards formaldehyde gas. ^{28,29} This was achieved by controlling the interlayer of the organic components, such as polyaniline (PANI), poly (5,6,7,8-tetrahydro-1-naphthylamine) (PTHNA), and poly-o-anisidine (PoANIS) while using a semiconductive host layer of MoO₃ deposited on an electrode surface. ²⁸ However, the sensor configuration required a certain time for formaldehyde molecules to diffuse through the organic layer to react with the MOS, leading to a delay in the sensor response. ²⁸ Wang et al. also developed organic-inorganic hybrid MoO_x/PANI nanowires and nanotubes with the potential for improving the conductivity for the detection of VOCs. ³⁰ Here we report a novel approach for the development of a formaldehyde-specific MOS, in which we hypothesized that a carbon support can enhance the dispersion of ultrasmall MoO_x nanoparticles resulting in an increased sensor response to VOCs. ³¹

In the current study, we focused on developing a molybdenum oxide (MoO_x)-based electrochemical sensor for the detection of formaldehyde in the gas phase. To boost the conductivity of the electrochemical sensor, 32 MoO_x nanoclusters were grafted to the oxygen-containing groups (i.e., carboxyl groups) of a highly conductive carbon. Cyclic voltammetry (CV) was used to measure the current change (ΔA) of the MoO_x/Carbon composite due to its reaction with formaldehyde gas. 33 In addition, electrochemical impedance spectroscopy (EIS) was used to gain a better understanding of the interaction between formaldehyde gas and MoO_x.

Experimental

Materials.—All the chemicals were obtained from Sigma-Aldrich, USA, except for cycloheptatriene molybdenum tricarbonyl ((C_7H_8)Mo(CO)₃) (Strem Chemicals, USA) and Vulcan XCmax22 (Cabot, USA). Cycloheptatriene molybdenum tricarbonyl (99%, airsensitive material), n-pentane (anhydrous, 99+%), and Vulcan XCmax22 were used to synthesize the MoO_x/Carbon nanocomposites inside a glove box. Nitric acid (ACS reagent, 90%) was used to functionalize Vulcan XCmax22, which is a highly conductive carbon. A commercial formaldehyde solution (ACS reagent, 37 wt% in H_2O , containing 10–15 wt% of methanol), ethyl alcohol

¹Department of Chemical Engineering, The University of Toledo, Toledo, Ohio, United States of America

²711th Human Performance Wing, Air Force Research Laboratory, Wright-Patterson AFB, Ohio, United States of America ³Department of Materials Science and Engineering, The Ohio State University, Columbus, Ohio, United States of America

(anhydrous, 200 proof, 99.5%), methanol (ACS reagent, 99.9%), acetone (ACS reagent, 99.5%), and 2-propanol (anhydrous, 99.5%) were used for investigating the sensor selectivity. Formic acid (puriss. p.a., ACS reagent, Ph. Eur. ≥98%) was used to study the detection mechanism. Screen-printed electrodes (SPGEs, Pine Research Instrumentation, Inc., USA) with a 2 mm gold working electrode, Ag/AgCl reference electrode, and Pt counter electrode were used as base transducers. SPGEs were pretreated in a mild piranha solution containing 1:3 (v/v) hydrogen peroxide solution (30 wt%) and sulfuric acid (99.99%) for 10 min. A Nafion 117 containing solution (~5% in a mixture of lower aliphatic alcohols and water) was used as a solid-state ionic electrolyte. Molybdenum (VI) oxide (99.7% trace metals basis) was also used for preparing a physical mixture with acid-treated Vulcan XCmax22 carbon. A Gamry Reference 600 potentiostat (Gamry Instruments, USA) was used to perform cyclic voltammetry (CV) and electrochemical impedance spectroscopy (EIS). A EuroCellTM Standard glass cell (Gamry Instruments, USA) was used as a test chamber for the detection experiments. An Elitech GSP-6 probe (Elitech Technology, Inc., USA) was used to monitor the temperature and humidity inside the chamber. Industrial-grade nitrogen (Airgas, USA) was used to provide the baseline of the CV and EIS measurements, as well as the carrier gas. Additionally, industrialgrade argon (Airgas, USA) was used to regulate the humidity inside the gas chamber, as this gas allows for control of humidity fluctuations. After demonstrating the effectiveness of our sensor for the detection of formaldehyde in inert atmosphere, the system was modified to use breathing air (O.E. Meyer, USA) as the carrier gas and for control of the humidity inside the gas chamber.

Functionalization of the carbon support.—Highly conductive Vulcan XCmax22 carbon was functionalized with a HNO₃ solution to create oxygen-containing groups on its surface (i.e., carboxyl groups). These groups act as the anchoring points for grafting of the molybdenum precursor, cycloheptatriene molybdenum tricarbonyl, (C_7H_8)Mo(CO)₃, to the carbon surface. For acid treatment, 10 g of carbon was added into a round-bottom flask, which was placed inside a silicone oil bath at 105 °C. After adding 175 ml of 5 M HNO₃ solution to the flask, this was immediately connected to a distillation column refrigerated at -10 °C to perform the acid treatment under reflux. After stirring for 4 h, the acid-treated carbon was filtered and washed with DI water several times until neutral pH. Finally, the acid-treated carbon was dried overnight in an oven at 60 °C and stored at room temperature.

Synthesis of the MoO_x/Carbon nanocomposites.—MoO_x is considered an n-type semiconductor, as most of the charge carriers are electrons. The electron charge carriers could reduce the oxidized VOCs causing a decrease in the MOS conductivity. MoO_x consists of octahedral units, each of them containing six oxygen atoms and a molybdenum atom at the center;³⁶ and the formaldehyde molecule contains a carbon atom connected to an oxygen atom through a double bond.³² The hydrogen bonding occurs between Mo-O in MoOx, which is more electronegatively charged, and H-CO of formaldehyde. There is also a nucleophilic interaction between Mo-O in MoO_x and the H-C=O group of formaldehyde, which makes MoO_x more selective towards CH₂O. ^{37,38} For the synthesis of MoO_x/Carbon nanocomposites, the acid-treated carbon (1 g) was placed in a Schlenk tube, which was immersed in a silicone oil bath at 105 °C. The Schlenk tube was then connected to a Schlenk line under vacuum for 24 h to remove moisture. After drying, the Schlenk tube was filled with argon and brought inside a glove box filled with UHP argon for synthesizing the MoO_x/Carbon nanocomposite by surface organometallic chemistry (SOMC),³⁹ as shown in Fig. 1. The amount of molybdenum precursor (cycloheptatriene molybdenum tricarbonyl) used was varied to synthesize a series of nanocomposites with different Mo loadings, being these of 0.149, 0.315, and 0.710 g for the synthesis of 5, 10, and 20 wt% Mo/ Carbon, respectively. The desired amount of molybdenum precursor

was dissolved in 15 ml of n-pentane inside a glove box and stirred for 30 min. After that, the precursor solution was added into the Schlenk tube containing 1 g of acid-treated carbon. After 12 h of stirring for efficient linkage of the molybdenum precursor to the carboxyl groups, the Schlenk tube was sealed and connected to the Schlenk line to dry n-pentane out. Once dried, the Schlenk tube was connected to a gas line under 10 ml min $^{-1}$ flow of nitrogen. Then, the tube was placed inside a tubular oven where the temperature was increased until 400 °C at 5 °C min $^{-1}$. The sample was then held at 400 °C for 2 h before cooling down to room temperature under a flow of nitrogen. This step contributes to the removal of the precursor ligands to obtain $\text{MoO}_x/\text{Carbon}$ nanocomposite was then collected and stored in a desiccator at room temperature. All the $\text{MoO}_x/\text{Carbon}$ nanocomposites were labeled as 5, 10, and 20 wt% Mo/Carbon to indicate the theoretical Mo loading.

Deposition of MoO₂/Carbon nanocomposite onto the electrode for the detection of formaldehyde.—Screen-printed gold electrodes (SPGEs) were cleansed with a 0.1 M H₂SO₄ solution using CV in the potential range from -0.8 to 0.8 V with a scan rate of 100 mV s⁻¹. After that, 50 mg of MoO₂/Carbon nanocomposite was suspended in 2.5 ml of DI water. The solution was then sonicated for 1 h and deposited onto the working electrode of the SPGE by delivering a single drop (2.5 μ l) using a micropipette. The droplet was then dried in an oven at 60 °C for 20 min. Two additional single droplets with intermediate drying were added to generate the MoO_x/Carbon nanocomposite layer on the SPGE. After that, 2.5 ul of Nafion solution was added on top of the MoO₂/Carbon nanocomposite and dried in air for 20 min. Even when the thickness of the two different layers was not measured, these should be consistent throughout all the electrodes as the same volumes of MoO_x/Carbon and Nafion solutions were delivered. The SPGE modified with a layer of MoO_x/Carbon and a second layer of Nafion (Nafion-MoO_x/Carbon-SPGE) was used as the electrochemical sensor for the detection of formaldehyde gas by CV and EIS.

Chamber testing.—The experimental setup for the detection of formaldehyde gas was designed in our lab as shown in Fig. 2. A commercial thermocouple with a humidity probe was connected to a 270 ml glass chamber, as shown in Figs. 2a, 2b, to monitor the temperature and humidity during the experiment. Then, moist argon gas was flowed into the chamber via the gas tube shown in Fig. 2c to control the humidity by adjusting the flow rate of argon. This gas allowed for an excellent control of the humidity without fluctuations. Through the fourth neck, nitrogen and formaldehyde gases were flowed into the chamber as demonstrated in Fig. 2d. The concentration of formaldehyde in the gas phase was controlled by dilution of the formaldehyde solution with DI water before feeding it into the chamber, and the gas phase concentration of FA in the chamber was estimated using Aspen Plus simulation software. Argon and nitrogen were flowed into the chamber unit after obtaining the desired humidity. Gases were vented out through a small gap between the sensor and the chamber, and a pressure gauge was used to ensure that there was no pressure buildup. Nafion-MoO_x/Carbon-SPGE, which was connected to a Gamry Reference 600 potentiostat, was inserted into the chamber as shown in Fig. 2e for the detection of formaldehyde gas and other VOCs. Before running the experiments, the conditions in the chamber were set at the desired relative humidity (RH) with 25 ± 1 °C. To do so, 10 ml min⁻¹ of nitrogen was flowed into the chamber first. Then, the first CV and EIS experiments were run to investigate the response of the Nafion-MoO_x/Carbon-SPGE to nitrogen. These results were used as the baseline for the calculation of the sensor response to formaldehyde gas. After that, a predetermined concentration of formaldehyde gas was flowed into the chamber and the second CV and EIS were recorded to monitor the response Nafion-MoO_x/Carbon-SPGE. Finally, nitrogen was flowed again to purge formaldehyde gas out of the chamber, and the third CV and

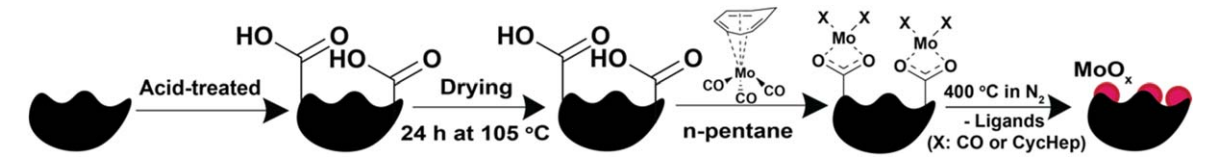


Figure 1. Illustration of the synthesis of the MoO_x/Carbon nanocomposites.

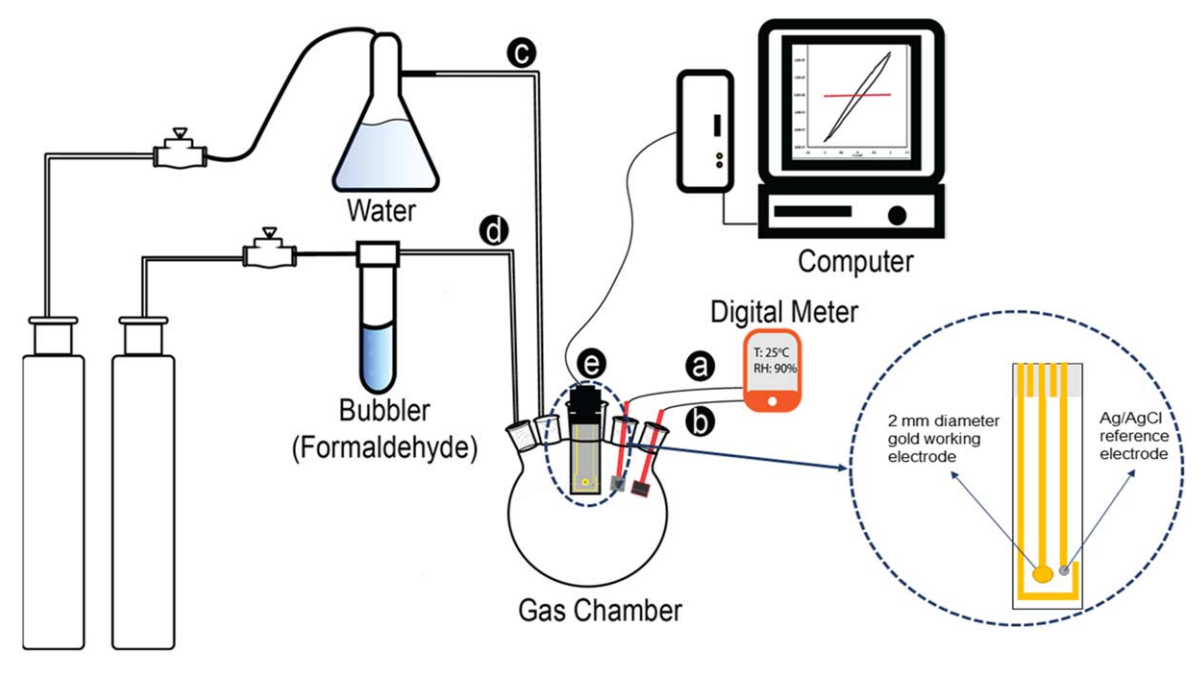


Figure 2. Schematic diagram of the experimental setup for the detection of formaldehyde.

EIS experiments were recorded to confirm the response of Nafion-MoO_x/Carbon-SPGE to nitrogen, and thus, study the reversibility of the measurements. The experiments were repeated multiple times with different sensors to verify the consistency of the sensor response by flowing nitrogen and different concentrations of formaldehyde gas. CV experiments were recorded in the range of -1.0 to 1.0 V with 50 mV s⁻¹ scan rate because these parameters provided consistent current signals. The resulting cyclic voltammograms were used to calculate the current change (ΔA) due to the electrochemical reaction between the composite sensor and formaldehyde gas. The ΔA was calculated using the procedure described in Fig. 3, in which ΔA is taken from the difference between the currents at -1.0 and 1.0 V. On the other hand, EIS measurements were recorded in the ranges of 5 to 1000 Hz and 0.1 to 0.01 Hz with AC and DC voltages of 40 and 0.001 mV, respectively. After confirming the effectiveness of our electrochemical method for the detection of formaldehyde in inert atmosphere, the experimental setup shown in Fig. 2 was modified to use breathing air in both lines (carrier gas and control of the humidity), as the ultimate goal is to develop a sensor capable of measuring formaldehyde under atmospheric conditions.

Characterization of the MoO_x/Carbon nanocomposites.—An FTS-4000 Varian Excalibur Series Fourier-transform infrared (FTIR) spectrometer was used to investigate the functionalization of the carbon surface upon acid treatment and the linkage of the molybdenum precursor. To do so, 1.2 mg of dried sample was blended with 500 mg of dried KBr. Then, 5 mg of the blended sample was pressed into a thin pellet. FTIR spectra were recorded in the range of 450–4000 cm⁻¹. A TA Instruments Q50 thermogravimetric analysis (TGA) equipment was used to determine the required temperature for removal of the ligands of the organometallic precursor and to confirm the success of the acid treatment and the

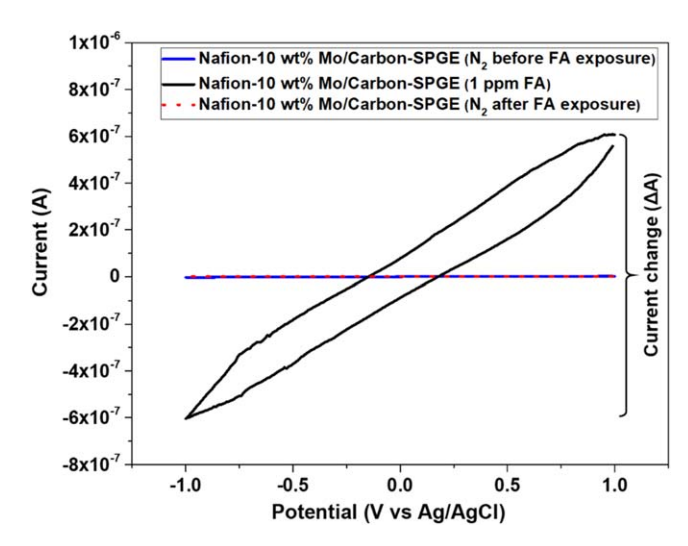


Figure 3. Current change (ΔA) obtained with Nafion-10 wt% Mo/Carbon-SPGE when exposed to FA (90% RH).

anchorage of the Mo precursor to the carbon surface. For TGA, 7 mg of the sample was loaded into an aluminum plate and the temperature was ramped (10 °C min⁻¹) from 25 to 1100 °C under 50 ml min⁻¹ of nitrogen. Additionally, we conducted inductively coupled plasma optical emission spectrometry (ICP-OES) analyses to determine the actual molybdenum loading on carbon. These analyses were performed by Galbraith Laboratories, Inc. using a PerkinElmer Optima 5300 V ICP-OES. Prior to analysis, the samples were fused with sodium peroxide over a Bunsen burner and dissolved in water before being acidified. Scanning transmission

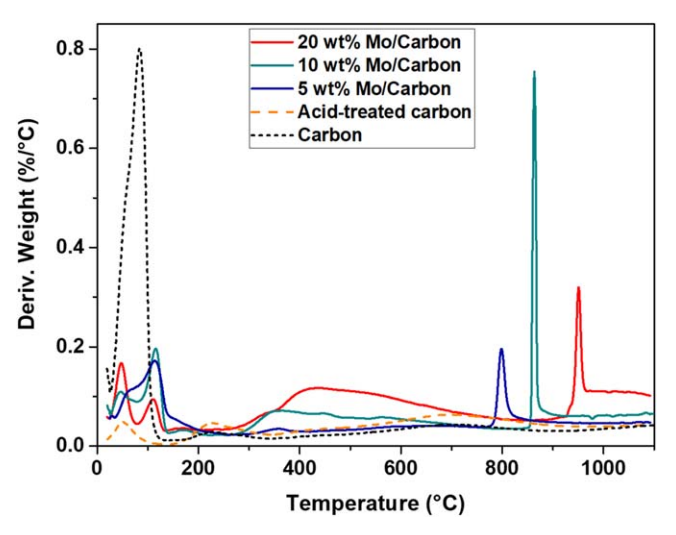


Figure 4. Thermogravimetric analyses of carbon, acid-treated carbon, 5, 10, and 20 wt% Mo/Carbon before thermal treatment for ligands removal.

Table I. Theoretical and actual Mo loading determined by ICP-OES.

Sample (theoretical Mo loading)	Actual Mo loading (wt%)	
5 wt% Mo/Carbon	7.4	
10 wt% Mo/Carbon	12.7	
20 wt% Mo/Carbon	19.5	

electron microscopy (STEM) was also used to determine the distribution of MoO_x onto the carbon surface. For the preparation of the TEM specimens, the nanocomposite powders were dispersed in ethanol, sonicated for 10 min, and then deposited onto 300-mesh copper TEM grids coated with lacey carbon films. High-angle annular dark-field (HAADF) STEM images were carried out at 300 kV using a FEI Titan^{3TM} G2 60–300 S/TEM with a collection angle of 106-200 mrad to ensure proper Z-contrast. Compositional information was collected via energy-dispersive X-ray spectroscopy (EDS) mapping using a Super-X EDS detector on the FEI Titan³ G2 60-300 S/TEMequipped with a high coherence, high brightness, and field emission electron gun (X-FEG). A low probe current and fast acquisition were utilized to minimize the electron beam effect to preserve the pristine structures. X-ray photoelectron spectroscopy (XPS) data were collected in a Kratos Axis Ultra XPS equipment using a monochromated Al source (1486.6 eV) and a charge neutralizer. The XPS resolution was about 0.6 eV when the pass energy of 20 eV was used. The energy scale was calibrated with Ag 3d_{5/2} that was assigned at 368.21 eV. The samples were also characterized by X-ray diffraction (XRD) using a Rigaku Ultima III diffractometer equipped with a CuK α X-ray generator (1 = 1.54 Å) and a slit collimation system operated in the Bragg-Brentano mode. The scan was performed over a 2θ angle range of 10° to 110° continuously at a rate of 1° min⁻¹. Acquired data were analyzed using the JADE Pro software package (Materials Data Inc., Livermore, CA, USA).

Results and Discussion

Synthesis and characterization of MoO_x /Carbon nanocomposites.—Nanocomposites with three different MoO_x loadings were synthesized by using surface organometallic chemistry (SOMC)⁴⁰: 5, 10, and 20 wt% Mo/Carbon. As previously stated, the highly conductive carbon was first functionalized to create anchoring points for grafting of the molybdenum precursor. Successful functionalization of carbon was demonstrated by FTIR (Fig. S1 (available online at stacks.iop.org/JES/168/067525/mmedia) in the Supplementary

Material). Figure S1a shows the spectrum obtained with pristine Vulcan XCmax22 carbon, where the absorption bands at 667 and 2300-2400 cm⁻¹ are assigned to atmospheric CO₂ in the FTIR chamber. 41 After the acid treatment (Fig. S1b), the FTIR spectrum shows additional absorption bands, which represent the oxidized carbon surface. The additional bands at $\sim 1250\,\mathrm{cm}^{-1}$ and $3200-3600\,\mathrm{cm}^{-1}$ represent the –OH in-plane bending and stretching vibrations, respectively.⁴¹ Moreover, the absorption bands at 1591 cm⁻¹ can be attributed to the C=C stretching vibration.⁴² Interestingly, the oxidized carbon also shows a strong band at 1733 cm⁻¹, which is associated with the C=O stretching vibration of carboxyl groups, 43 indicating the successful functionalization of carbon upon the acid treatment. When adding 5 wt% Mo to the acidtreated carbon (Fig. S1c), the FTIR spectrum hardly changed, likely due to the low loading of Mo precursor. However, when 10 and 20 wt% Mo were added to carbon, most of the bands associated with the carboxyl groups were reduced because of the grafting of the molybdenum precursor. Unlike the synthesis of the 5 wt% Mo/ Carbon nanocomposite, in which the solution of the precursor became clear after 12 h, in the synthesis of the 10 and 20 wt% Mo/Carbon samples, the solution still showed a bright orange and red-orange color, respectively, after 12 h, which indicated incomplete uptake of the molybdenum precursor by carbon. This would confirm an excess of precursor with respect to the number of carboxyl groups available for linkage. Therefore, upon solvent removal, the organometallic molybdenum precursor would stay physically adsorbed on carbon without proper linkage to the surface. These results are in agreement with those obtained by thermogravimetric analysis (TGA).

TGA was performed to determine the temperature required to remove the ligands of the organometallic precursor. Figure 4 shows the derivative weight loss with respect to the temperature. When comparing the weight loss at ~ 100 °C on carbon and the acid-treated carbon, it can be concluded that the water content was higher in pristine carbon. The additional derivative weight loss at 220 °C could be assigned to the elimination of the carboxyl groups, 44 which demonstrates the successful functionalization of carbon. Additionally, all the MoO_x/Carbon nanocomposites showed a weight loss at 800 °C or above, which is assigned to the decomposition of the Mo precursor grafted to the carbon surface. As can be seen in Fig. 4, while the decomposition of the 5 wt% Mo/Carbon sample takes place at 800 °C, it happens at higher temperatures for 10 and 20 wt% Mo, which could be due to increased stability associated with higher precursor loading. Additionally, the intensity of the weight loss for 10 wt% Mo/Carbon is higher than that of the 5 wt% Mo/Carbon sample, which is attributed to the higher loading of Mo precursor anchored to the surface. Remarkably, the intensity of the weight loss with the 20 wt% Mo/Carbon nanocomposite is lower; however, there is a broad evolution between 300 °C and 700 °C that could be attributed to physisorbed or weakly adsorbed precursor on the carbon surface. In fact, that evolution also appears to some extent with the 10 wt% Mo/Carbon sample, which might already indicate the depletion of the carboxyl groups on the carbon surface through the binding of the precursor.

A good correlation between theoretical and actual Mo loading was confirmed by ICP-OES analysis, being these of 7.4, 12.7, and 19.5 wt% Mo for theoretical 5, 10, and 15 wt% Mo, respectively (Table I). STEM images (Fig. 5) and EDS elemental mapping (Fig. S2) were also collected to study the dispersion of the MoO_x nanoparticles onto the carbon surface. The 10 wt% Mo/Carbon nanocomposite exhibited a uniform dispersion of MoO_x on the carbon support, as observed in Figs. 5a–5c. The advantage of small-size MoO_x nanoparticles is a large surface area for the sensor to react with the target gas. The STEM images also showed that increasing the MoO_x loading to 20 wt% Mo promoted the aggregation of the nanoparticles (Figs. 5d–5f), which is undesired as it reduces the surface area for the detection of formaldehyde. Even when the 20 wt% Mo/Carbon sample showed MoO_x nanoparticles of larger size, these were not large enough to provide additional information by

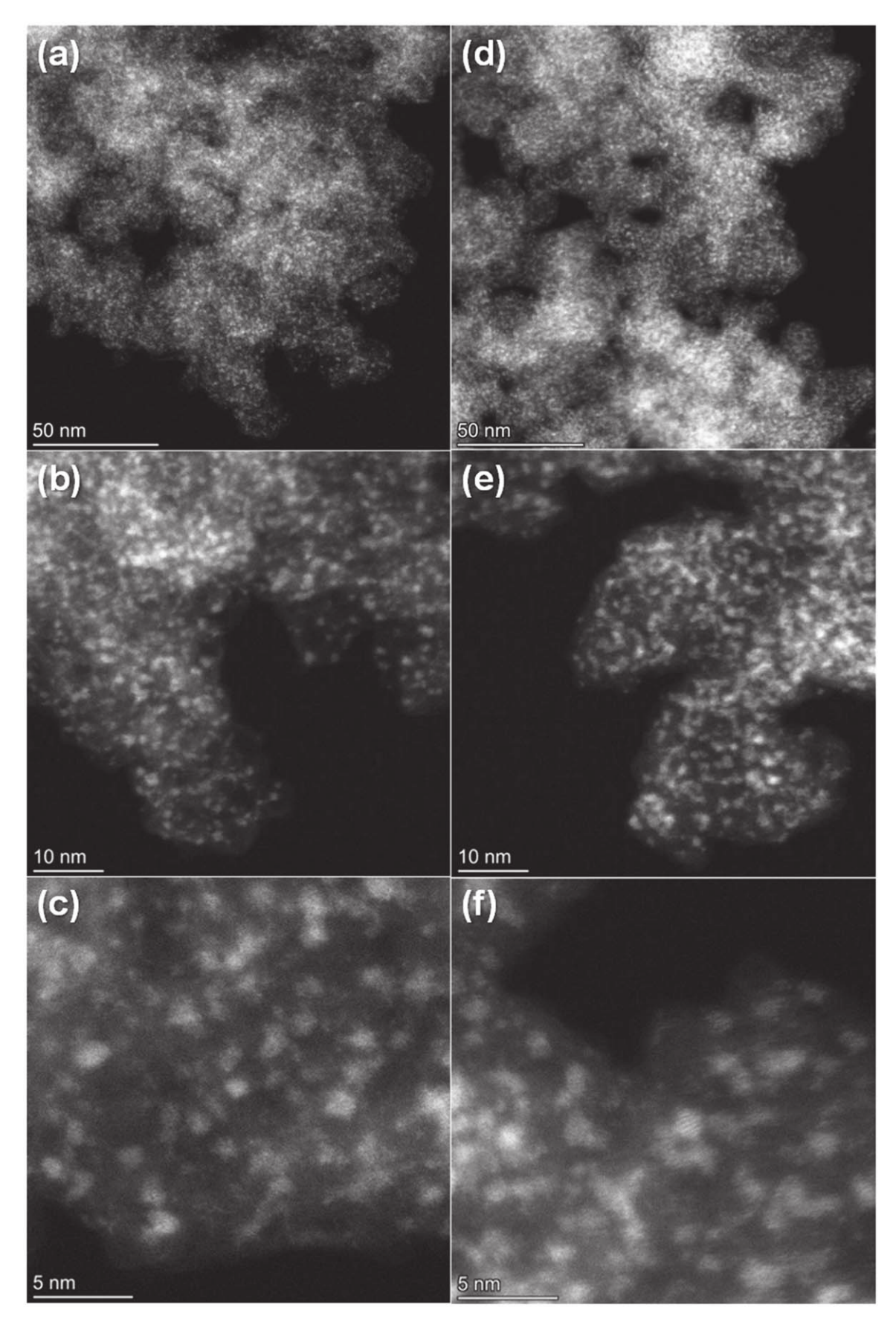


Figure 5. STEM images of (a)–(c) 10 wt% and (d)–(f) 20 wt% Mo/Carbon nanocomposites.

XRD, as the diffractogram was very similar to that obtained with acid-treated carbon (Fig. S3). The peaks observed in all cases

corresponded to the (002), (101), and (110) planes of the graphitic structure. 45,46 The samples were also characterized by XPS to study the nature of the molybdenum species on the carbon surface. Figure S4 shows the Mo 3d and O 1 s XPS spectra obtained with the 10 and 20 wt% Mo/Carbon samples. The Mo $3d_{5/2}$ peak at 232.35 eV confirmed the presence of molybdenum on the surface as MoO₃.

Effect of the relative humidity on the sensor response.—As the sensor operates at room temperature, it seems necessary to study the effect of the relative humidity (RH) on the sensor response. Figure 6 shows the current change obtained with the Nafion-10 wt% Mo/Carbon-SPGE toward 1 ppm of formaldehyde gas. As it can be seen in Fig. 6, the relative humidity in the testing chamber had a great impact on the sensitivity of the electrochemical gas sensor, obtaining the highest current change at RH of 90%. For that reason, we selected 90% relative humidity to perform all the experiments here reported.

Effect of Nafion on the gold electrode.—Nafion contributes to the adhesion of the $MoO_x/Carbon$ nanocomposite to the electrode surface. Which enables the conduction of protons and permits the access of formaldehyde gas to the MoO_x surface. Furthermore, humidity has an influence on the Nafion permeability, which increases as the water content rises, which would explain the higher sensor response obtained at high RH. The major advantage of Nafion is that it can conduct O_2 and O_2 and O_3 are room temperature and it can work as a solid-state electrolyte in which formaldehyde gas is dissolved.

Effect of the different layers on the gold electrode.—In order to investigate the influence of each laver Nafion-MoO_x/Carbon-SPGE, the sensor response was measured independently with every single layer as shown in Fig. S5. In these experiments, nitrogen was used as a control to verify the selectivity of the Nafion-MoO_x/Carbon-SPGE toward formaldehyde gas. As stated in the experimental section, CV and EIS experiments were performed under a constant flow rate of nitrogen or VOCs (10 ml min⁻¹) at room temperature with 90% RH. First, cyclic voltammograms of a bare SPGE, an electrode modified with the acid-treated carbon, and an electrode modified with Nafion were compared in the detection of nitrogen and formaldehyde gas as shown in Fig. S5. As expected, all of them presented negligible sensor responses (6-8 pA) to nitrogen, and there was still no response after flowing formaldehyde gas into the testing chamber. These results are due to the lack of MoO_x on the electrode for the detection of formaldehyde gas. The same experimental trend was observed when conducting EIS experiments (Fig. S6), with the bare SPGE, acid-treated carbon-SPGE, and Nafion-SPGE showing the same impedances in the presence of formaldehyde gas or when flowing nitrogen before or after exposure to FA, which indicated that the impedance was unaffected by formaldehyde. Therefore, we confirmed that the bare SPGE and the electrode modified with acidtreated carbon or Nafion do not significantly interact with formaldehyde gas. Consequently, we concluded that MoO_x was essential for the detection of formaldehyde.

Effect of the MoO_x loading and dispersion on the sensor response.—The sensor response to 0.1 ppm of formaldehyde gas with 5, 10, and 20 wt% Mo/Carbon nanocomposites is shown in Fig. 7a. While the Nafion-5 wt% Mo/Carbon-SPGE showed a ΔA of 0.323 μA ppm $^{-1}$, Nafion-10 and 20 wt% Mo/Carbon-SPGE showed 5.10 and 0.122 μA ppm $^{-1}$, respectively. The Nafion-5 wt% Mo/Carbon-SPGE showed lower ΔA to formaldehyde gas than Nafion-10 wt% Mo/Carbon-SPGE due to the lower loading of the sensing element (MoO_x). Similarly, the Nafion-20 wt% Mo/Carbon-SPGE showed the lowest ΔA of the series, likely due to the high degree of aggregation of the MoO_x nanoparticles that resulted in a small surface area to react with formaldehyde. The effect of the MoO_x loading on the degree of aggregation was observed in the STEM

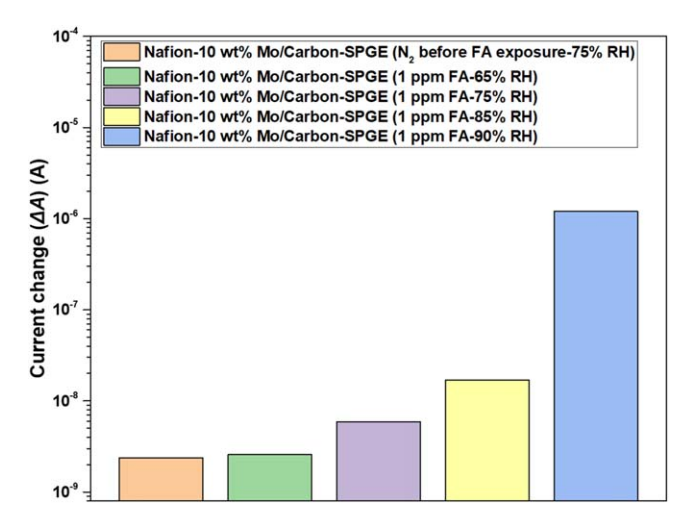


Figure 6. Current change (ΔA) obtained with Nafion-10 wt% Mo/Carbon-SPGE when exposed to 1 ppm FA under different values of relative humidity (RH).

images shown in Fig. 5. The maximum ΔA to formaldehyde gas was obtained with the 10 wt% Mo/Carbon nanocomposite, which could be attributed to the higher surface area from the homogeneous dispersion of MoO_x nanoparticles on the carbon surface. To further study the effect of the synthesis method and the dispersion of MoO_x on the sensitivity of the sensor, we synthesized another composite by the physical mixture of commercial MoO₃ and acid-treated carbon with a theoretical 10 wt% Mo loading. As shown in Fig. 7b, this composite provided a smaller ΔA of 0.0063 μA compared to the 10 wt% Mo/Carbon nanocomposite synthesized by SOMC, which further highlights the importance of the synthesis method and the high dispersion obtained with nanosized MoO_x.

Gas sensing properties of Nafion-10 wt% Mo/Carbon-SPGE.— Once we identified the optimum MoO_x loading in the nanocomposite for the detection of formaldehyde, we investigated the sensor response of Nafion-10 wt% Mo/Carbon-SPGE towards different concentrations of formaldehyde gas. To achieve that, the Nafion-10 wt% Mo/Carbon-SPGE was exposed to 0.0025, 0.005, 0.01, 0.1, and 1 ppm formaldehyde gas as shown in Fig. 8. These gas-phase concentrations were obtained by bubbling 25 ml aqueous solutions of formaldehyde using a gas flow rate of 10 ml min⁻¹. Those aqueous solutions were prepared in 100 ml volumetric flasks by diluting different volumes of the commercial formaldehyde solution (ACS reagent, 37 wt% in H₂O, containing 10–15 wt% of methanol) in DI water, being those volumes of 0.004, 0.008, 0.0166, 0.166, and 1.49 ml, respectively. As expected, the highest ΔA was obtained when exposing the gas sensor to 1 ppm of formaldehyde gas (1.20) μ A), followed by 0.503, 0.295, 0.0256, and 0.00512 μ A with 0.1, 0.01, 0.005, and 0.0025 ppm of formaldehyde gas, respectively. The relationship between the current change (ΔA) and the formaldehyde concentration is shown in Fig. S7. It is worth mentioning that the ΔA with Nafion-10 wt% Mo/Carbon-SPGE significantly increased in the presence of formaldehyde when compared to the bare SPGE, acidtreated carbon-SPGE, and Nafion-SPGE, as shown in Fig. S5. Moreover, ΔA with Nafion-10 wt% Mo/Carbon-SPGE instantly dropped after switching back to N2, which indicated a rapid sensor response and recovery to formaldehyde gas. We concluded that the Nafion-10 wt% Mo/Carbon-SPGE was able to detect the presence of formaldehyde in this experimental setup at concentrations as low as 0.06 ppm (60 ppb) with the sensor response being generated from the interaction between MoO_x and formaldehyde gas. This limit of detection (LOD) (60 ppb) was calculated using the equation LOD = $(3.3 \times SD)/b$, ⁵¹ in which SD and b represent the standard deviation of the blank (N2) and the slope of the regression line in Fig. S7, respectively. The LOD obtained with Nafion-10 wt% Mo/Carbon-

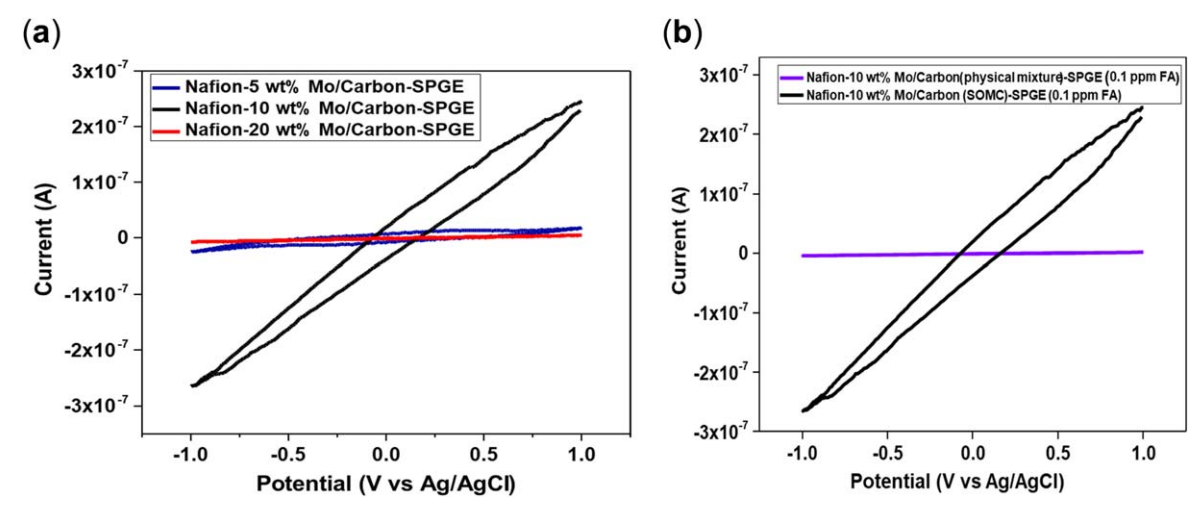


Figure 7. Cyclic voltammograms: (a) Nafion-5, 10, and 20 wt% Mo/Carbon-SPGE to 0.1 ppm of FA; (b) Nafion-10 wt% Mo/Carbon-SPGE by SOMC vs physical mixture to 0.1 ppm of FA gas (90% RH).

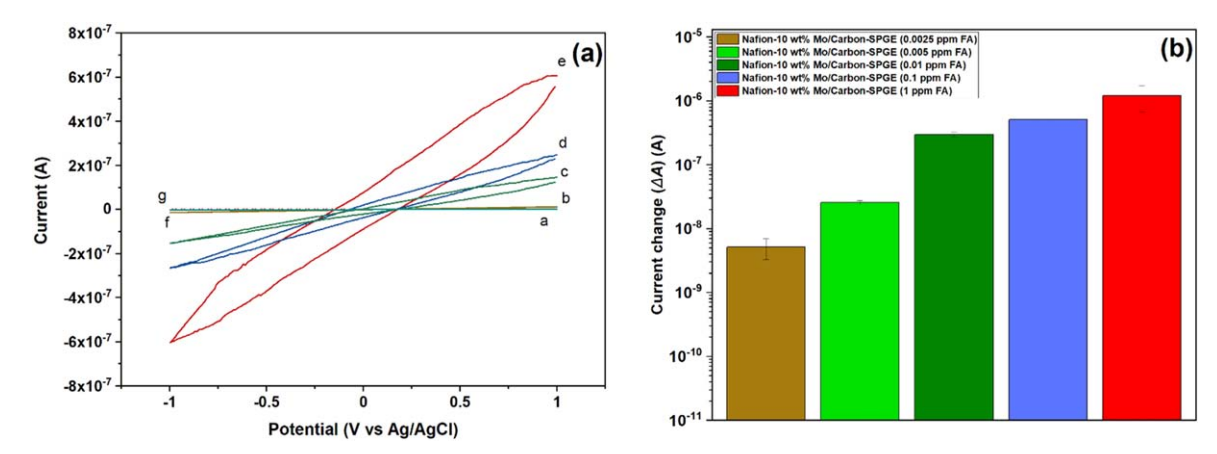


Figure 8. (a) Cyclic voltammetry (CV) results and (b) current change (ΔA) obtained at 90% RH with Nafion-10 wt% Mo/Carbon-SPGE for N₂ before formaldehyde exposure (control, CV curve a), N₂ after formaldehyde exposure (recovery, CV curve b), 0.01 ppm (CV curve c), 0.1 ppm (CV curve d), 1 ppm (CV curve e), 0.005 ppm (CV curve f), and 0.0025 ppm of FA (CV curve g). The error bars represent the standard deviation of three CV cycles.

SPGE was lower than others reported in the literature for MoO₃-based sensors, which were in the range of 1–100 ppm, as shown in Table II. Furthermore, the Nafion-10 wt% Mo/Carbon-SPGE was used for the detection of formaldehyde for six consecutive cycles. This experiment provided a consistent sensor response, thus confirming the stability and reusability of the sensor for the detection of formaldehyde gas.

Electrochemical impedance spectroscopy (EIS) measurements are able to identify changes in the interfacial properties of a surface-modified electrode. A low frequency of 6 Hz was used to study the impedance changes on the surface of Nafion-10 wt% Mo/Carbon-SPGE. As can be seen in Figs. 9b, 9d, 9f, the sensor impedance decreased with increased concentration of formaldehyde gas, being these of 9.88, 7.52, and 3.79 M Ω in the presence of 0.01, 0.1, and 1 ppm of formaldehyde at 6 Hz, respectively. Even though the measured impedance with Nafion-MoO_x/Carbon-SPGE was high

for a metal-oxide gas sensor, these results demonstrated the possibility of using EIS to detect formaldehyde gas based on the impedance change. The higher sensor impedance with 0.01 ppm formaldehyde is due to a limited interaction between the low concentration of formaldehyde and MoO_x on the electrode surface, which causes a lack of electron transfer at the electrode interface. As expected, the EIS results showed the same trend as CV, with the sensor resistance decreasing with an increase in the concentration of formaldehyde gas.

One of the most important parameters in the development of sensors is the selectivity towards a target molecule. In this work, we also studied the selectivity of our Nafion-10 wt% Mo/Carbon-SPGE to different VOCs. Figure 10 shows the sensor response to 0.1 ppm of acetone, ethanol, methanol, isopropyl alcohol, and formaldehyde measured independently. Remarkably, the ΔA of Nafion-10 wt% Mo/Carbon-SPGE toward 0.1 ppm of formaldehyde was more than

Table II. Comparative table of the LODs reported in the literature for the electrochemical detection of formaldehyde gas.

Sensor	Operating temperature	LOD (ppm)	References.
MoO ₃ microsheets	275 °C	100	52
Ni-doped α-MoO ₃	225 °C	3	33
Pt-decorated MoO ₃ nanowires	Room temperature	1	53
Nafion-MoO _x /Carbon	Room temperature	0.06	This work

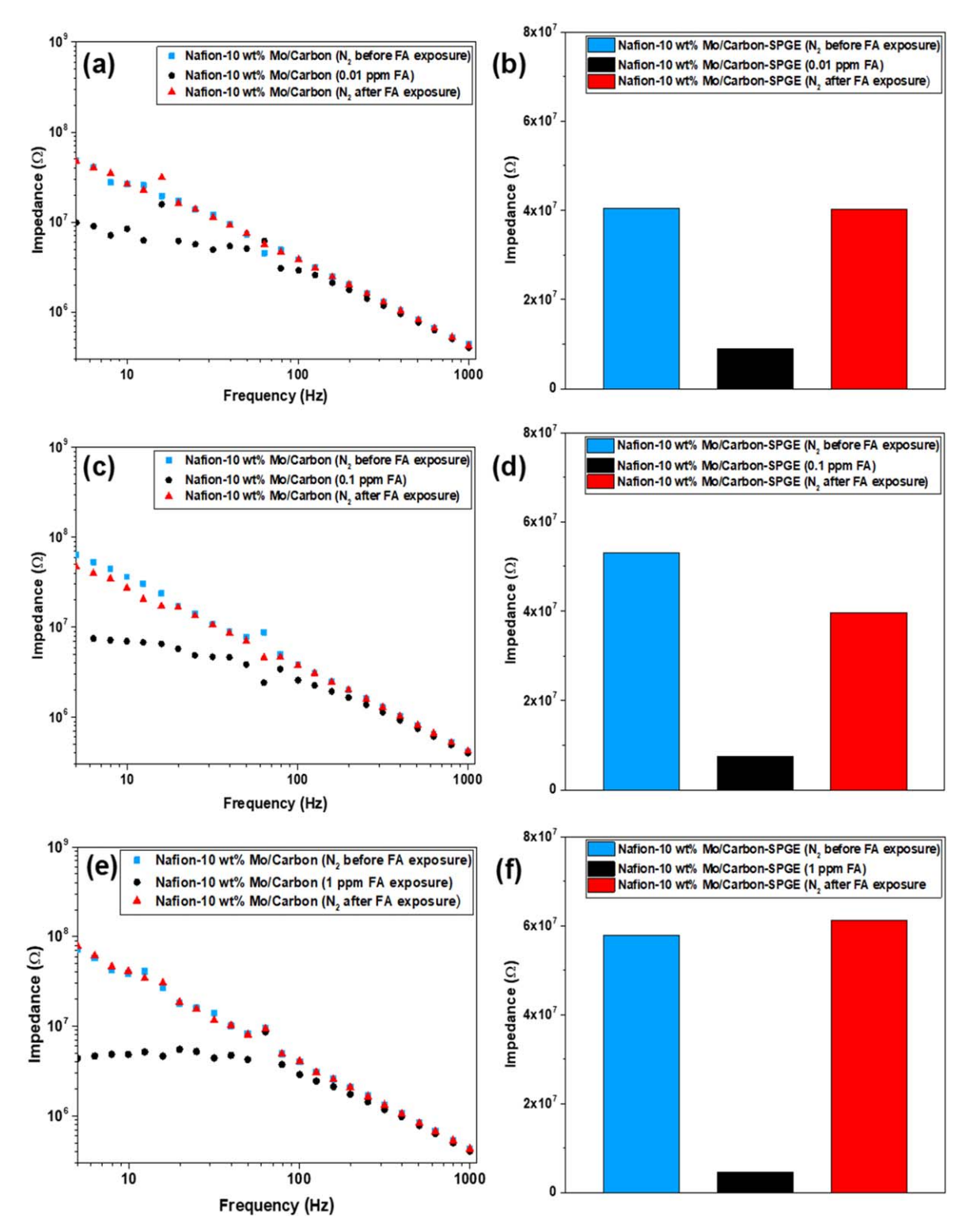


Figure 9. Electrochemical impedance spectroscopy (EIS) results and sensor impedance at 6 Hz with Nafion-10 wt% Mo/Carbon-SPGE to (a), (b) 0.01 ppm, (c), (d) 0.1 ppm, and (e), (f) 1 ppm of formaldehyde with N₂ flow before and after FA exposure (90% RH).

an order of magnitude higher than those of methanol and isopropyl alcohol, and more than two orders of magnitude higher than acetone and ethanol. The significant difference in the ΔA of formaldehyde as a target gas compared to other VOCs implies that the Nafion-10 wt% Mo/Carbon-SPGE has an excellent selectivity towards formaldehyde gas even at low concentrations with an insignificant sensor response towards other VOCs. These results confirmed that MoOx is a

promising sensing element for the selective electrochemical detection of formaldehyde.

Nyquist plots using a Nafion-10 wt% Mo/Carbon-SPGE.—The interaction between Nafion-10 wt% Mo/Carbon-SPGE and formal-dehyde gas was also investigated using EIS. Figure 11e illustrates the Nyquist plots obtained from the faradaic impedance spectra with the response of Nafion-10 wt% Mo/Carbon-SPGE towards different

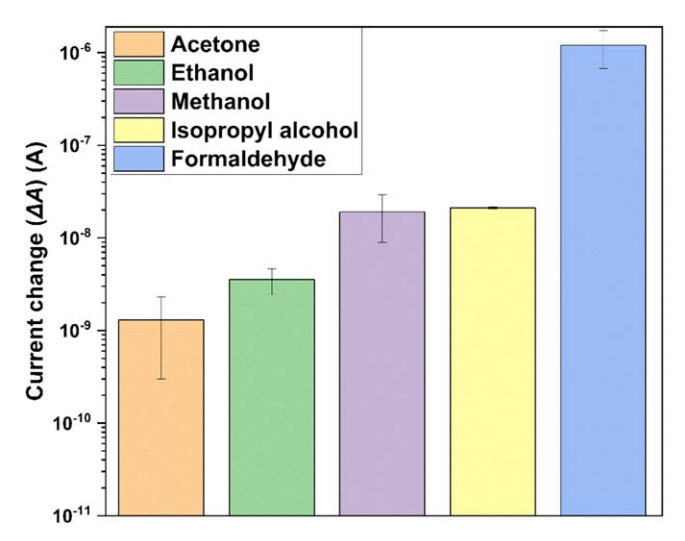


Figure 10. Sensor responses with Nafion-10 wt% Mo/Carbon-SPGE towards 0.1 ppm of acetone, ethanol, methanol, isopropyl alcohol, and formaldehyde (90% RH). The error bars represent the standard deviation of three CV cycles.

concentrations of formaldehyde. All Nyquist plots with 0.01, 0.1, and 1 ppm formaldehyde gas show a semicircle at a high frequency that represents the charge transfer resistance, which implies that there is no diffusion limitation when using Nafion-10 wt% Mo/Carbon-SPGE in the detection of formaldehyde. The diameter of the semicircles at high frequencies increases when decreasing the concentration of formaldehyde gas, which shows the same trend as cyclic voltammograms (Fig. 8) and Bode plots (Fig. 9a) in terms of the sensor impedance, i.e., the sensor impedance decreases as the concentration of formaldehyde gas increases. These results suggest that the Nafion-10 wt% Mo/Carbon-SPGE is not only able to detect formaldehyde but it can also provide its concentration.

Bode plots and the phase angle shifts of bare SPGE, acid-treated carbon-SPGE, and Nafion-SPGE were also recorded in order to estimate the electrical behavior on the electrode surface towards nitrogen and formaldehyde gases (Figs. 11a, 11b). The path of the Bode plots shows unaffected impedance to nitrogen and formaldehyde at both low and high frequencies, as shown in Fig. 11a. Moreover, bare SPGE, carbon-SPGE, and Nafion-SPGE show the same profiles of phase angle change for both nitrogen and formaldehyde gases (Fig. 11b). Thus, these results confirm that the electrochemical sensor has no response to formaldehyde gas in the absence of the MoO_x sensing element. However, once that the electrochemical sensor is modified with 10 wt% Mo (as MoO_x) (Nafion-10 wt% Mo/Carbon-SPGE), the sensor response to formaldehyde gas is completely different from that with bare SPGE, carbon-SPGE, and Nafion-SPGE. As displayed in Figs. 11c, 11d, the sensor resistance and the phase angle change vary according to the concentration of formaldehyde gas. However, there is not a significant distinction of phase angle shift for formaldehyde as compared to nitrogen in the range of 5 to 1000 Hz. Therefore, EIS was measured at lower frequencies ranging from 0.01 to 0.1 Hz to investigate and identify the phase angle shift of formaldehyde gas on Nafion-10 wt% Mo/Carbon-SPGE. Figure 11e shows the Nyquist plots for the responses of Nafion-10 wt% Mo/Carbon-SPGE to 0.01, 0.1, and 1 ppm FA. As the FA concentration decreases, the semicircle radius increases, which indicates greater resistances from the sensor. As no linear part was observed at lower frequencies, the mass diffusion-limited electron transfer process, which is represented as the Warburg impedance, seems to be negligible. The impedance diagrams have been fitted to the equivalent electrical circuit shown in the inset of Fig. 11e. The following electronic parameters were chosen in the circuit: R_u was measured between the working and reference electrodes, Rp is the charge transfer resistance, and CPE represents a constant phase element that simulates a non-ideal behavior of the capacitor so that CPE corresponds to the outer interface, which can be explained by the roughness and non-homogeneity of the surface of the electrode. $R_{\rm p}$ is inversely proportional to the electron transfer rate, and $W_{\rm d}$ is a finite length Warburg element that represents the diffusion of ions from the Nafion layer to the surface of the MoO_x-modified electrode. The full semicircles demonstrate a stable response of the sensor. As shown in Fig. 11f, there is no phase angle shift at low frequencies when using untargeted compounds (methanol, isopropyl alcohol, and nitrogen). However, Nafion-10 wt% Mo/Carbon-SPGE shows a noteworthy phase angle shift at 0.05 Hz in the presence of formaldehyde. The appearance of a phase angle shift at 0.05 Hz proves the high selectivity of the Nafion-10 wt% Mo/Carbon-SPGE towards formaldehyde.

Proposed mechanism for the gas sensor.—The cyclic voltammograms displayed in Fig. 8 demonstrated the interaction between the surface of the Nafion-10 wt% Mo/Carbon-SPGE and formaldehyde gas. A highly conductive carbon was used as the support for the dispersion of MoO_x nanoclusters to boost the conductivity of our sensor. The reaction of MoO_x on the surface of the electrochemical sensor with formaldehyde gas results in an increase in the sensor conductivity referred to as current change (ΔA). However, further investigation is needed to verify the oxidation and reduction mechanisms of formaldehyde on the MoO_x/Carbon composite. Additionally, the semicircle shape of the Nyquist plots (Fig. 11e) seems to indicate the formation of a by-product. Supplementary high-performance liquid chromatography (HPLC) studies after CV when using Nafion-10 wt% Mo/Carbon-SPGE and a 50-ppm formaldehyde liquid solution confirmed the presence of formic acid (see Figs. S8 and S9 in Supplementary Material for details). Therefore, the proposed mechanism for the detection of formaldehyde by the Nafion-10 wt% Mo/Carbon-SPGE is the partial oxidation of FA to formic acid and the reduction of MoO_x (Fig. 12). This mechanism was also proposed by Danilevich et al. 55 for the oxidation of formaldehyde over another redox catalyst comprised of vanadia-titania oxide. They concluded that in the absence of oxygen, both methyl formate and traces of formic acid are obtained, while in the presence of oxygen, formic acid and carbon oxides are predominantly produced. They also stated that the addition of water increased the rate of formation of formic acid, which would be consistent with the high humidity required (90% RH) for effective detection. Additionally, as the detection was carried out in inert atmosphere, and not in the presence of O2 (or air), it would be expected to observe some deactivation after multiple uses due to the lack of oxygen sites (reduced MoO_x).⁵⁶ This fact, together with the desire of using the electrochemical sensor under atmospheric conditions, brought us to evaluate the sensitivity and selectivity of the nanocomposite towards formaldehyde in air, as this would make it more appropriate for common use with the added advantage of MoOx regeneration and prolonged activity.

Detection of formaldehyde under atmospheric conditions.—Figures 13 and S10 confirmed the effectiveness of Nafion-10 wt% Mo/Carbon-SPGE for the detection of formaldehyde gas in air. As can be seen in Fig. 13, the current responses were similar to those obtained under inert atmosphere, especially at higher FA concentrations (0.1 and 1 ppm FA). Remarkably, when using the electrochemical sensor for the detection of 1 ppm FA in air, a prominent oxidation peak was observed at around 0.7 V, which further supports the reaction mechanism discussed above.

Conclusions

MoO_x/Carbon nanocomposites were successfully synthesized by using surface organometallic chemistry (SOMC) and were characterized by FTIR, TGA, XRD, STEM, EDS, XPS, and ICP-OES.

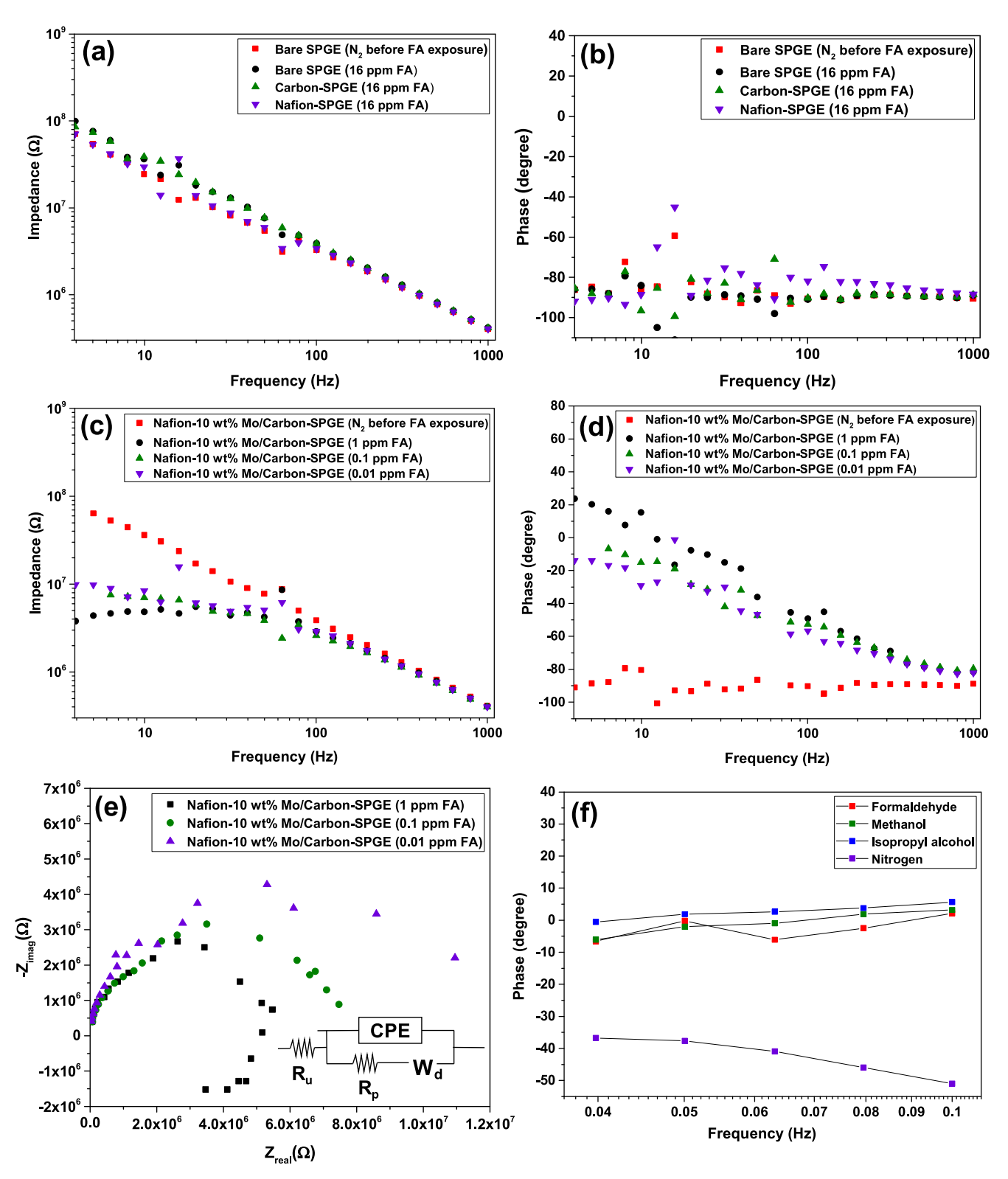


Figure 11. Bode plots obtained with (a), (b) bare SPGE, Carbon-SPGE, and Nafion-SPGE, and (c), (d) Nafion-10 wt% Mo/Carbon-SPGE. Nyquist plots at different FA concentrations (e) and phase angle shifts at different VOCs (f) with Nafion-10 wt% Mo/Carbon-SPGE (90% RH).

FTIR spectra showed successful functionalization of the carbon surface and anchorage of the organometallic precursor to the carboxyl groups on the carbon support. TGA provided the temperature necessary to decompose the ligands of the molybdenum precursor and allowed us to distinguish between physically and chemically adsorbed species. A gold electrode modified with a 10 wt % Mo/Carbon nanocomposite and Nafion provided a gas sensor with

high sensitivity and selectivity towards formaldehyde gas. The $\text{MoO}_x/\text{Carbon}$ nanocomposite gas sensor exhibited a higher response towards formaldehyde when compared to other VOCs, such as methanol, ethanol, acetone, and isopropyl alcohol. In addition, this nanocomposite sensor was able to detect concentrations of formal-dehyde as low as 60 ppb with a sensitivity of 5.13 μA ppm⁻¹. Even when this study only shows a proof of concept developed using N_2

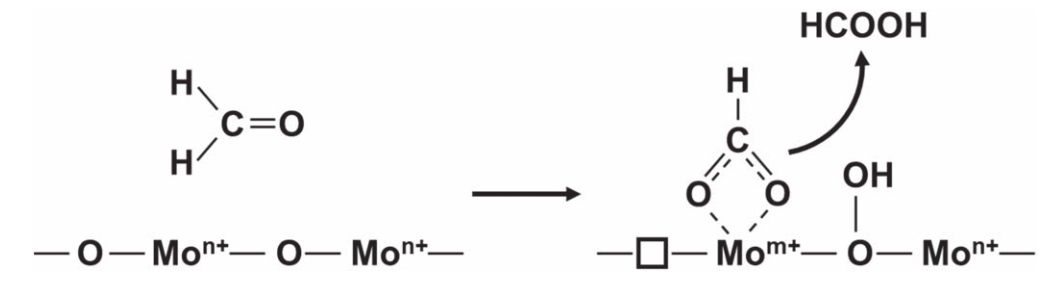


Figure 12. Proposed mechanism for the oxidation of formaldehyde into formic acid over MoO_x.

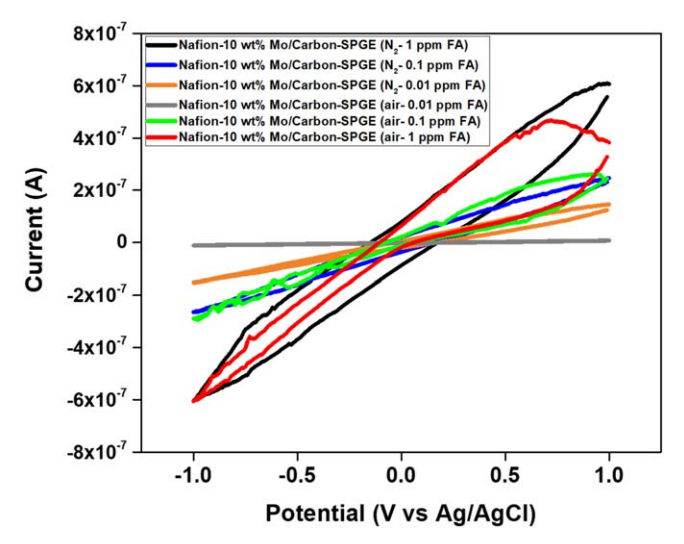


Figure 13. Cyclic voltammetry (CV) results obtained with Nafion-10 wt% Mo/Carbon-SPGE under inert (N2) and atmospheric (air) conditions when exposed to 0.01, 0.1, and 1 ppm of FA (90% RH).

as the carrier and high relative humidity, which are clear limitations for practical use, the results imply a promising future for the use of MoO_x-based electrochemical sensors for the detection of formaldehyde at room temperature. Future development should focus on studying the performance under various environmental conditions and exploring the use of more suitable ionic transfer compounds for operation at lower relative humidity.

Acknowledgments

This material is based upon work supported by the National Science Foundation under Grant No. 1817294. D.S.K. acknowledges support for the Air Force Summer Faculty Fellowship Program (SFFP) for his research stay at the 711th Human Performance Wing, Air Force Research Lab, to conduct research on this project. Electron microscopy was performed at the Center for Electron Microscopy and Analysis (CEMAS) at The Ohio State University. The authors also acknowledge the Michigan Center for Materials Characterization for the use of their XPS, acquired under NSF grant DMR-0420785, and Dr. Haiping Sun for technical support.

ORCID

Joerg R. Jinschek https://orcid.org/0000-0003-1574-0899 Ana C. Alba-Rubio https://orcid.org/0000-0002-1831-8338

References

- (2010), World Health Organization, 'WHO Guidelines for Indoor Air Quality: Selected Pollutants.' https://www.euro.who.int/__data/assets/pdf_file/0009/128169/
- 2. M. C. McCarthy, Y.-A. Aklilu, S. G. Brown, and D. A. Lyder, "Source apportionment of volatile organic compounds measured in Edmonton, Alberta." Atmos. Environ., 81, 504 (2013).
- 3. A. P. Jones, "Indoor air quality and health." Atmos. Environ., 33, 4535 (1999).

- 4. S. Sandler and R. Strom, "Determination of formaldehyde by gas chromatography." Anal. Chem., 32, 1890 (1960).
- O. Li, P. Sritharathikhun, and S. Motomizu, "Development of novel reagent for Hantzsch reaction for the determination of formaldehyde by spectrophotometry and fluorometry." Anal. Scien., 23, 413 (2007).
- 6. J. M. Lorrain, C. R. Fortune, and B. Dellinger, "Sampling and ion chromatographic
- determination of formaldehyde and acetaldehyde." *Anal. Chem.*, **53**, 1302 (1981).

 7. S. Kumar, V. Pavelyev, N. Tripathi, V. Platonov, P. Sharma, R. Ahmad, P. Mishra, and A. Khosla, "Review-recent advances in the development of carbon nanotubes based flexible sensors." J. Electrochem. Soc., 167, 047506 (2020).
- M. Masikini, M. Chowdhury, and O. Nemraoui, "Review-metal oxides: application in exhaled breath acetone chemiresistive sensors." J. Electrochem. Soc., 167, 037537 (2020).
- D. E. Williams, "Semiconducting oxides as gas-sensitive resistors." Sens. Actuators B: Chem., 57, 1 (1999).
- 10. N. Barsan, D. Koziej, and U. Weimar, "Metal oxide-based gas sensor research: how to?" Sens. Actuators B: Chem., 121, 18 (2007).
- 11. G. F. Fine, L. M. Cavanagh, A. Afonja, and R. Binions, "Metal oxide semiconductor gas sensors in environmental monitoring." Sensors, 10 (2010).
- 12. D. Zhang, Z. Liu, C. Li, T. Tang, X. Liu, S. Han, B. Lei, and C. Zhou, "Detection of NO2 down to ppb levels using individual and multiple In2O3 nanowire devices." Nano Lett., 4, 1919 (2004).
- 13. H. J. Park, N.-J. Choi, H. Kang, M. Y. Jung, J. W. Park, K. H. Park, and D.-S. Lee, "A ppb-level formaldehyde gas sensor based on CuO nanocubes prepared using a polyol process." Sens. Actuators B: Chem., 203, 282 (2014).
- 14. S.-J. Young et al., "Multi-walled carbon nanotubes decorated with silver nanoparticles for acetone gas sensing at room temperature." J. Electrochem. Soc., 167, . 167519 (2020).
- 15. W. Guo, "Hollow and porous ZnSnO3 gas sensor for ethanol gas detection." J. Electrochem. Soc., 163, B131 (2016).
- S. Das and M. Pal, "Review—non-invasive monitoring of human health by exhaled breath analysis: a comprehensive review." J. Electrochem. Soc., 167, 037562
- 17. I. Castro-Hurtado, J. Herrán, G. G. Mandayo, and E. Castaño, "SnO2-nanowires grown by catalytic oxidation of tin sputtered thin films for formaldehyde detection." Thin Solid Films, 520, 4792 (2012).
- 18. H. Park, Y. Chung, S. Lee, E. Lee, H. Ahn, S.-H. Kim, and D.-J. Kim, " VOC Gas Sensing Properties." SnO₂/Graphene Oxide Composites on J. Electrochem. Soc., 164, B690 (2017).
- 19. T. Chen, Q. J. Liu, Z. L. Zhou, and Y. D. Wang, "The fabrication and gas-sensing characteristics of the formaldehyde gas sensors with high sensitivity." Sens. Actuators B: Chem., 131, 301 (2008).
- N. Han, Y. Tian, X. Wu, and Y. Chen, "Improving humidity selectivity in formaldehyde gas sensing by a two-sensor array made of Ga-doped ZnO." Sens. Actuators B: Chem., 138, 228 (2009).
- 21. A. Kösemen, S. Öztürk, Z. Şen, Z. A. Kösemen, M. Harbeck, and Z. Z. Öztürk, "Volatile organic compounds and dimethyl methyl phosphonate (DMMP) sensing properties of the metal oxide functionalized QCM transducers at room temperature." J. Electrochem. Soc., 164, B657 (2017).
- 22. N. P. Rumjit, P. Thomas, C. W. Lai, and Y. H. Wong, "Review-recent advancements of ZnO/rGO nanocomposites (NCs) for electrochemical gas sensor
- applications." *J. Electrochem. Soc.*, **168**, 027506 (2021).

 23. X. Wang, F. Cui, J. Lin, B. Ding, J. Yu, and S. S. Al-Deyab, "Functionalized nanoporous TiO2 fibers on quartz crystal microbalance platform for formaldehyde sensor." Sens. Actuators B: Chem., 171-172, 658 (2012).
- (2000), United States Environmental Protection Agency, 'Health Effects Notebook for Hazardous Air Pollutants' https://www.epa.gov/sites/production/files/2016-09/ documents/formaldehyde.pdf.
- 25. E. K. W. Tan, G. Rughoobur, J. Rubio-Lara, N. Tiwale, Z. Xiao, C. A. B. Davidson, C. R. Lowe, and L. G. Occhipinti, "Nanofabrication of conductive metallic structures on elastomeric materials." Sci. Rep., 8, 6607 (2018).
- K. Subodh, Prakash, and D. T. Masram, "Chromogenic covalent organic polymerbased microspheres as solid-state gas sensor." J. Mater. Chem. C, 8, 9201 (2020).
- 27. T. Itoh, I. Matsubara, W. Shin, N. Izu, and M. Nishibori, "XPS study of organic/MoO₃ hybrid thin films for aldehyde gas sensors: correlation between average Mo valence and sensitivity." *J. Ceram. Soc. Jpn.*, **118**, 171 (2010).
- I. Matsubara, T. Itoh, W. Shin, N. Izu, and M. Nishibori, "Characterization of intercalation type organic/MoO₃ nanohybrids and their VOC sensing properties." Adv. Mater. Res., 47-50, 1514 (2008).

- T. Itoh, I. Matsubara, W. Shin, N. Izu, and M. Nishibori, "Highly aldehyde gassensing responsiveness and selectivity of layered organic-guest/MoO₃-host hybrid sensor." *J. Ceram. Soc. Jpn.*, 115, 742 (2007).
- S. Wang, Q. Gao, Y. Zhang, J. Gao, X. Sun, and Y. Tang, "Controllable synthesis
 of organic-inorganic hybrid MoOx/polyaniline nanowires and nanotubes."

 Chem.-Eur., 17, 1465 (2011).
- E. Auer, A. Freund, J. Pietsch, and T. Tacke, "Carbons as supports for industrial precious metal catalysts." Appl. Catal. A: Gen., 173, 259 (1998).
- H. Chhina, S. Campbell, and O. Kesler, "An oxidation-resistant indium tin oxide catalyst support for proton exchange membrane fuel cells." *J. Power Sources*, 161, 893 (2006).
- J. Shen, S. Guo, C. Chen, L. Sun, S. Wen, Y. Chen, and S. Ruan, "Synthesis of Nidoped α-MoO₃ nanolamella and their improved gas sensing properties." *Sens. Actuators B: Chem.*, 252, 757 (2017).
- J. Li, L. Ma, X. Li, C. Lu, and H. Liu, "Effect of nitric acid pretreatment on the properties of activated carbon and supported palladium catalysts." *Ind. Eng. Chem.* Res., 44, 5478 (2005).
- G. de la Puente, A. Centeno, A. Gil, and P. Grange, "Interactions between molybdenum and activated carbons on the preparation of activated carbonsupported molybdenum catalysts." J. Colloid Interface Sci., 202, 155 (1998).
- T. He and J. Yao, "Photochromism of molybdenum oxide." J. Photochem. Photobiol., C, 4, 125 (2003).
- J. Wang, I. Matsubara, N. Murayama, S. Woosuck, and N. Izu, "The preparation of polyaniline intercalated MoO₃ thin film and its sensitivity to volatile organic compounds." *Thin Solid Films*, 514, 329 (2006).
- (2021), National Library of Medicine, National Center for Biotechnology Information, 'Database' https://pubchem.ncbi.nlm.nih.gov/compound/712.
- C. Copéret, "Single-sites and nanoparticles at tailored interfaces prepared via surface organometallic chemistry from thermolytic molecular precursors." Acc. Chem. Res., 52, 1697 (2019).
- J. M. Notestein, E. Iglesia, and A. Katz, "Grafted metallocalixarenes as single-site surface organometallic catalysts." J. Am. Chem. Soc., 126, 16478 (2004).
- W. Chen, F. Cazier, F. Tittel, and D. Boucher, "Measurements of benzene concentration by difference-frequency laser absorption spectroscopy." *Appl. Opt.*, 39, 6238 (2000).
- Z. Lin, L. Ji, and X. Zhang, "Electrodeposition of platinum nanoparticles onto carbon nanofibers for electrocatalytic oxidation of methanol." *Mater. Lett.*, 63, 2115 (2009).
- J.-H. Zhang, T. Zhu, N. Li, and C.-W. Xu, "Glycerol electrooxidation on Au supported on carbon spheres by Stöber method in alkaline medium." *Int. J. Electrochem. Sci.*, 8, 9508 (2013).

- S. A. Chernyak, A. S. Ivanov, N. E. Strokova, K. I. Maslakov, S. V. Savilov, and V. V. Lunin, "Mechanism of thermal defunctionalization of oxidized carbon nanotubes." *J. Phys. Chem. C*, 120, 17465 (2016).
- Y. Ma, H. Wang, S. Ji, J. Goh, H. Feng, and R. Wang, "Highly active vulcan carbon composite for oxygen reduction reaction in alkaline medium." *Electrochim. Acta*, 133, 391 (2014)
- M. Carmo, A. R. dos Santos, J. G. R. Poco, and M. Linardi, "Physical and electrochemical evaluation of commercial carbon black as electrocatalysts supports for DMFC." *J. Power Sources*, 173, 860 (2007).
- S. Guimond, D. Göbke, J. M. Sturm, Y. Romanyshyn, H. Kuhlenbeck, M. Cavalleri, and H.-J. Freund, "Well-ordered molybdenum oxide layers on Au(111): preparation and properties." *J. Phys. Chem. C*, 117, 8746 (2013).
- L. Rassaei, F. Marken, M. Sillanpää, M. Amiri, C. M. Cirtiu, and M. Sillanpää, "Nanoparticles in electrochemical sensors for environmental monitoring." *TrAC*, *Trends Anal. Chem.*, 30, 1704 (2011).
- R. J. Mortimer and A. Beech, "AC impedance characteristics of solid-state planar electrochemical carbon monoxide sensors with Nafion" as solid polymer electrolyte." *Electrochim. Acta*, 47, 3383 (2002).
- P.-A. Gross, T. Jaramillo, and B. Pruitt, "Cyclic-voltammetry-based solid-state gas sensor for methane and other VOC detection." *Anal. Chem.*, 90, 6102 (2018).
- A. Shrivastava and V. Gupta, "Methods for the determination of limit of detection and limit of quantitation of the analytical methods,." *Chron. Young Sci.*, 2, 21 (2011).
- 52. W. Jiang, D. Wei, S. Zhang, X. Chuai, P. Sun, F. Liu, Y. Xu, Y. Gao, X. Liang, and G. Lu, ""The facile synthesis of MoO₃ microsheets and their excellent gas-sensing performance toward triethylamine: high selectivity, excellent stability and superior repeatability." New J. Chem., 42, 15111 (2018).
- X. Fu et al., "Ultra-fast and highly selective room-temperature formaldehyde gas sensing of Pt-decorated MoO₃ nanobelts." J. Alloys Compd., 797, 666 (2019).
- 54. B.-W. Park, D.-Y. Yoon, and D.-S. Kim, "Formation and modification of a binary self-assembled monolayer on a nano-structured gold electrode and its structural characterization by electrochemical impedance spectroscopy." *J. Electroanal. Chem.*, 661, 329 (2011).
- E. V. Danilevich, G. Y. Popova, I. A. Zolotarskii, A. Ermakova, and T. V. Andrushkevich, "Kinetics of formaldehyde oxidation on a vanadia-titania catalyst." *Catal. Ind.*, 2, 320 (2010).
- M. Ai, "The reaction of formaldehyde on various metal oxide catalysts." J. Catal., 83, 141 (1983).